

Recombination Dynamics of Charge Pairs in a Push–Pull Polyfluorene-Derivative

Simon Gélinas,^{*,†,‡} James Kirkpatrick,[§] Ian A. Howard,^{||} Kerr Johnson,[‡] Mark W. B. Wilson,[‡] Giuseppina Pace,[‡] Richard H. Friend,[‡] and Carlos Silva[†]

[†]Département de Physique & Regroupement Québécois sur les Matériaux de Pointe, Université de Montréal, C.P. 6128, Succursale Centre-Ville, Montréal, Québec H3C 3J7, Canada

[‡]Cavendish Laboratory, University of Cambridge, J.J. Thompson Avenue, Cambridge CB3 0HE, United Kingdom

[§]Oxford Martin School, University of Oxford, Oxford OX1 2JD, United Kingdom

^{||}Max Planck Institute for Polymer Research, D-55128 Mainz, Germany

S Supporting Information

ABSTRACT: We investigate the properties of long-lived species in F8BT films through time-resolved photoluminescence (PL) measurements at room temperature and 10 K. The kinetics consist of an initial exponential decay ($\tau = 2.26$ ns) followed by a weak power-law decay ($I(t) \propto t^{-1}$) up to at least 1 ms, both of which depend weakly on temperature. From fluence-dependent PL and ultrafast transient absorption (TA) measurements, we confirm that this emission arises from the recombination of geminate charge-pairs generated through singlet–singlet annihilation. This behavior is a consequence of the donor–acceptor nature of this polymer, which enhances singlet–singlet annihilation and facilitates the formation of long-lived geminate-pairs from energetic singlet states.

In recent years, the development of higher-efficiency organic-solar-cells has been driven by the design of ever-more-complicated push–pull-type polymers, which have strong donor–acceptor character (D–A) to harvest a broader portion of the solar spectrum.^{1,2} Much still needs to be understood on the properties of charges in these polymers before relations can be made to the macroscopic behavior of devices.^{3,4} We address this question by studying a model system that is one of the simplest D–A polymers available, F8BT, and that is also extensively characterized (see Figure 1 for chemical structure).^{5–7} We will focus on the kinetics of charges following photogeneration, as there is already a large number of studies on the nature and yield of charge generation in neat polymers.^{8–13} To do so, we optically generate charges and investigate how they recombine into singlet excitons using photoluminescence (PL) and transient-absorption measurements. More specifically, we use intense femtosecond laser pulses ($>1 \mu\text{J}/\text{cm}^2$) to generate charges through sequential photon absorption and bimolecular annihilation of singlets.^{7,14} Since these charges are generated from high-energy states, they have access to large areas of the energetic landscape. This results in a broad distribution of lifetime observable as they recombine into luminescent singlet excitons.

Numerous studies have been carried out on similar polymers to understand how to relate the observed PL decay and the underlying physics.^{15–19} It is known that the absorption of a photon generates a singlet exciton (S_1), which will most likely decay radiatively to the ground state (S_0). Other decay pathways are intersystem crossing into triplet excitons (T_1)^{20,21} and separation into electrostatically bound elec-

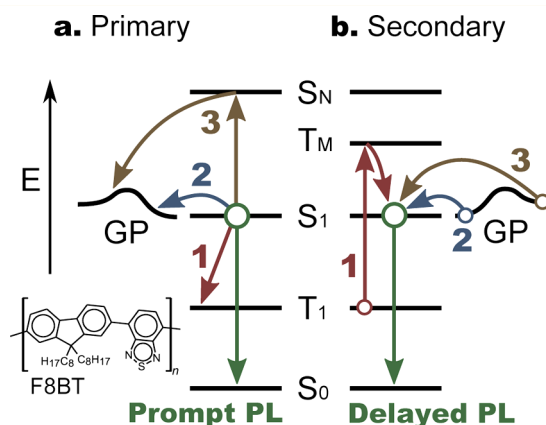


Figure 1. Chemical structure of F8BT and photophysical processes leading to PL (Green, $S_1 \rightarrow S_0 + h\nu$). (a) Prompt PL and primary processes following photoexcitation: (1) intersystem crossing into triplets (red, $S_1 \rightarrow T_1$), (2) geminate-pair formation (blue, $S_1 \rightarrow GP$), and (3) SSA (beige, $S_1 + S_1 \rightarrow S_N + S_0 \rightarrow GP + S_0$). (b) Delayed PL arising from secondary processes repopulating singlet excitons: (1) TTA (red, $T_1 + T_1 \rightarrow S_M + S_0 \rightarrow S_1 + S_0$), (2) GPR from thermally activated hopping (blue, $GP \rightarrow S_1$), and (3) through-space tunneling of geminate pair into singlet exciton (beige, $GP \rightarrow S_1$).

Special Issue: Paul F. Barbara Memorial Issue

Received: September 10, 2012

Revised: November 10, 2012

Published: November 14, 2012



tron–hole pairs (termed geminate pairs, GP). On time scales beyond the radiative lifetime of S_1 , faint singlet emission is generally observed and referred to as delayed luminescence. This can be ascribed to either triplet–triplet annihilation (TTA),^{15–18} where two T_1 interact with one another to generate an S_1 and an S_0 , or geminate-pair recombination (GPR),¹⁹ where a previously separated electron–hole-pair recombines into an exciton. Two different types of GPR must be distinguished. In the first one, the charges move by thermally activated hopping and eventually recombine due to their mutual Coulombic attraction. In the second case, recombination of the electron–hole pair is prevented by an energetic barrier, and recombination occurs through tunnelling. In the presence of an intense laser pulse, other nonlinear processes such as sequential photon absorption and singlet–singlet annihilation (SSA) generate high-energy singlet states (S_N).⁷ The former arises from excitations generated during the laser pulse that absorb a second photon from the same pulse, while the latter is caused by the high singlet density that leads to an enhanced collision-rate between singlets. Afterward, most S_N relax to S_1 within 100 fs²² except for a small fraction that form GPs.⁷ In the case of F8BT, we know that SSA is the dominant mechanism, while two-step excitation is negligible.^{7,23} All of these processes are summarized in Figure 1.

In order to relate this model to PL measurements, the processes presented in Figure 1 must be written quantitatively as a set of rate equations. These have been derived in the Supporting Information of this paper and elsewhere,^{15,17,18} but a brief qualitative overview is provided here. As the laser pulses we use are much faster than the timescales studied, we can assume that charges and triplets are generated instantaneously. In that case, the time-resolved kinetics and excitation-density dependence are rather well understood for both of these states.

For the TTA mechanism, there is an analytical model that describes the triplet exciton kinetics, including how triplets interact among themselves.^{15,17,18} From this model, we know that the probability of bimolecular interactions scales quadratically with the density of excited states, as the excitations need to diffuse in the bulk to meet one another. In the case of low triplet densities, the number of interactions is negligible, and the triplet population decays exponentially over time following $T_1(t) \propto e^{-t/\tau}$. As the density increases, bimolecular interactions become significant and eventually dominate the kinetics. This results in a power-law decay of the triplet population and the generation of singlet excitons as a byproduct, where $T_1(t) \propto t^{-1}$ and $S_1(t) \propto T_1(t)^2 \propto t^{-2}$. Since delayed S_1 emission originates from these collisions, it is expected to follow the same trend.^{15,17,18}

For the GPR mechanism, there is no density dependence as the electron and hole originate from the same exciton and recombine due to their mutual coulomb attraction. Their kinetics are not as straightforward as TTA but experiments and Monte Carlo simulations by Bassler et al. showed that they are expected to follow a $GP(t) \propto t^{-1}$ power-law.^{19,24} Brosseau et al. have also shown that these decays could be explained by a through-space tunneling of the electron–hole pair back into the singlet exciton.^{9,23,25,26} In that model, the local energetic landscape and the various separation distances between these e–h pairs lead to a distribution of GPR rates, resulting in a power-law decay where the slope reflects the spatial distribution of e–h separation.

We first show three low-temperature PL-spectra of the prompt (0–2 ns) and delayed emission (100 ns and 10 μ s after

photoexcitation) in the inset of Figure 2. The high-energy peak (2.25 eV) is associated with regions of increased planarity,

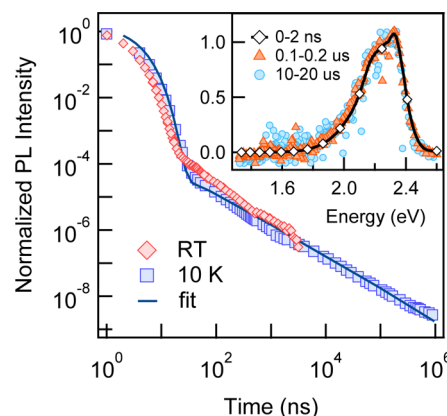


Figure 2. Normalized time-resolved PL of a F8BT film at RT and 10 K following excitation by 2.6 eV (475 nm) pulses at 5.4 μ J/cm². Inset: Normalized PL spectra of a F8BT film at 10 K integrated over the 0–2 ns (black line and diamonds), 0.1–0.2 μ s (orange triangles) and at 10–20 μ s (light-blue circles) windows following excitation.

where the BT unit stacks besides the F8 unit of the neighboring chain, whereas the low-energy peak (2.14 eV) arises from regions where the BT units are adjacent to one another and exhibit a higher torsional angle.^{5,6}

As the PL spectra do not change over time, we suspect that exciton-repopulation dynamics are similar in regions of both types of packing. Moreover, since the peak positions and spectral shapes remain unchanged over long time-scales, we conclude that there is no spectral diffusion. This then rules out the possibility of long-lived emission due to trapped excitons, as their lower-energy distribution would progressively lead to a broader and red-shifted PL spectrum. Interestingly, while phosphorescence has been documented to be ≈ 0.7 eV below the singlet for a wide variety of polyfluorenes,¹⁵ no signs of this process are present here.

To extend our understanding of these kinetic processes, we measure the spectrally integrated PL over time. These results, presented in Figure 2, show the decay of F8BT singlet emission at room temperature (RT) and 10 K. The measurements were carried out by exciting the sample with 2.6 eV laser-pulses at a fluence of 5.4 μ J/cm². The kinetics at both temperatures are composed of a fast exponential decay (prompt emission, $\tau = 2.26$ ns ± 0.02) followed by a power-law decay (delayed emission, $I(t) \propto t^{-1}$). There are only slight differences between both decays, where the room-temperature data show a slightly faster exponential decay and higher yield of long-lived emission.

Since we already understand the kinetics of the primary photoexcitations from previous publications,⁷ the relevant temporal regimes are readily identified. Then, instead of measuring the entire temporal kinetics, we only measure certain key temporal-regions and look at how they behave as a function of fluence (Φ). We will focus on two of them, the prompt and the delayed PL (80 ns to 1 μ s). While the former is a strong signal that accounts for the near-totality of the PL, the latter is a faint signal observable only by gating an intensified CCD over the specified time-window.

We present the fluence-dependence of the integrated PL-intensity of those time-regions in Figure 3. The prompt emission at room-temperature and 10 K is linear ($I(\Phi) \propto \Phi$)

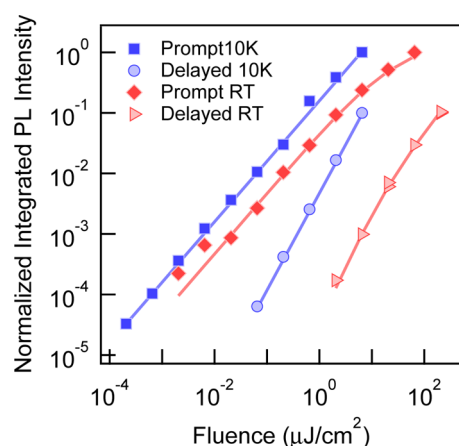


Figure 3. Normalized relative integrated and delayed (80 ns–1 μ s) PL intensities of a F8BT film measured at various fluences (Φ). The plain-lines are fits to the SSA model presented in eqs 1 and 2.

for most fluences. Only the higher-fluence region at RT shows a slight deviation after $\Phi = 1 \mu\text{J}/\text{cm}^2$, which has been attributed to SSA in previous publications.^{7,23,27} Contrasting with the linear behavior of the prompt PL, the delayed emission appears to follow a steeper power-law ($I(\Phi) \propto \Phi^{1.5}$). This superlinear behavior of the delayed PL implies that the regeneration mechanism is of bimolecular nature, suggesting it could arise from TTA.³¹ However, it is important to note that if the GPs were generated by a bimolecular process, such behavior could be accounted for.

Geminate and separated electron–hole pairs can indeed be produced by bimolecular interactions; we know from previous studies that charges in F8BT are byproducts of SSA, which occurs at high excitation densities.^{7,14} SSA happens when two excitons are in close vicinity, 4 nm or less in F8BT,⁷ and one of them undergoes Förster resonant energy transfer into the other. This can occur when two excitons are photogenerated next to each-other, in which case the annihilation happens within femtoseconds and is referred to as Förster-type SSA. By contrast, if the diffusion of excitons through the medium is required for them to collide and annihilate, the process is named diffusion-limited SSA and occurs on much longer time scales. Fortunately, the SSA threshold can be easily identified as the point at which the prompt singlet emission saturates as this process becomes significant. This leads to an effective reduction of the S_1 lifetime, which in turn reduces the time available for singlets to undergo intersystem crossing into triplets. It is thus expected that after reaching this threshold, the formation of triplets is quenched while the amount of GPs keeps growing. The prompt PL emission, $I_{\text{PL}}(\Phi)$, can be expressed as¹⁴

$$I_{\text{PL}}(\Phi) \propto \frac{1}{\beta\tau} \log(1 + \beta\tau\Phi) \quad (1)$$

where Φ is the fluence, τ the monomolecular lifetime (2.3 ns), and β is the bimolecular annihilation rate of singlets (SSA). From eq 1, the total amount of high-energy-singlet generated from SSA is

$$S_{\text{N}}(\Phi) \propto \frac{1}{2} \left(\Phi - \frac{1}{\beta\tau} \log(1 + \beta\tau\Phi) \right) \quad (2)$$

Since GP formation arising from SSA is proportional to the amount of S_{N} created, eq 2 also represents the fluence-dependence of delayed-luminescence induced by GPs. At low

fluences, the generation of GP is quadratic until $\Phi \approx (\beta\tau)^{-1}$, where it gradually kinks and becomes linear at higher fluences as any additional exciton are annihilated with a unity yield. The apparent $\Phi^{1.5}$ observed for delayed luminescence is simply this broad transition region between the two regimes. We fit this model to the prompt RT data presented in Figure 3 and plot the resulting power dependence. The 10 K data was not fitted to this model as the prompt-PL kink was not observed; power-laws were used instead. From eq 1 and 2, we know that the behavior of the delayed luminescence is entirely predicted by the parameters extracted from the prompt fit. This results in a nearly perfect fit, in agreement with previous measurements by Stevens et al.,⁷ without requiring the addition of any free parameter.

To confirm these findings, we investigated the fluence-dependent generation of long-lived states at RT with ultrafast transient-absorption spectroscopy (TA). In Figure 4 a, we plot

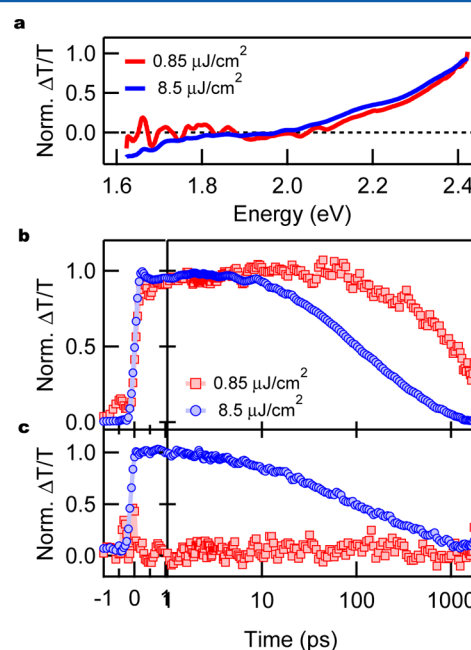


Figure 4. TA measurements at RT following excitation at 248 eV (500 nm) with pulses of $0.85 \mu\text{J}/\text{cm}^2$ (red) and $8.5 \mu\text{J}/\text{cm}^2$ (blue). (a) Normalized spectra integrated over 1–10 ps. (b) Normalized kinetics of the 2.17–2.41 eV feature (Stimulated emission of singlet excitons). (c) Normalized kinetics of the 1.63–1.77 eV feature (Photoinduced absorption of charges).

the time-integrated spectra of the 1–10 ps region following excitation at 248 eV with fluences of $0.85 \mu\text{J}/\text{cm}^2$ (red, $2.1 \times 10^{17} S_1/\text{cm}^3$, peak $\Delta T/T = 3.6 \times 10^{-4}$) and $8.5 \mu\text{J}/\text{cm}^2$ (blue, $2.1 \times 10^{18} S_1/\text{cm}^3$, peak $\Delta T/T = 3.6 \times 10^{-3}$). The high-energy feature (2.17–2.41 eV) is stimulated emission from singlet excitons whereas the low-energy feature (1.63–1.77 eV) can be photoinduced absorption from triplets or charges, but not from singlet as they absorb at 1.3 eV.^{7,23} The amplitude of these signals is directly proportional to the population of these excited states. Interestingly, we only observe the low-energy feature at high excitation densities or when exposed to air (not shown). These observations confirm that the 1.6 eV signature is not from triplets, as T_1 are quenched by oxygen while their generation is not fluence-dependent.²⁸

We then characterize the origin of this peak by measuring the fluence-dependent kinetics of the singlet exciton population

and present the results in Figure 4b. The high-fluence decay is characterized by an instrument-limited (100 fs) initial decay due to Förster-type SSA and a slower, nonexponential decay due to diffusion-limited SSA. As the charge population increases, the decay of excitons is accelerated by singlet-charge collisions where the exciton is annihilated. The low-fluence kinetics offer a sharp contrast where no initial decay is seen and where the lifetime is closer to the expected value of 2.3 ns. We then look at the 1.6 eV kinetics, shown in Figure 4c, which are relatively fast and highly nonexponential. Since the T_1 lifetime is $\approx 2.1 \mu\text{s}$ at RT,²⁰ the 1.6 eV feature observed here is entirely due to charge pairs. Moreover, as the decay starts within the first picosecond and differ significantly from the S_1 decay, it suggests that most charge pairs are formed relatively closely to one-another and recombine geminately.^{23,25} Looking at longer time scales, we observe a combination of two entangled mechanisms: the generation of GPs from diffusion-limited SSA and their recombination into S_1 . We conclude that GPs are formed by SSA and that GPR is the source of delayed luminescence.

Now that we have fully portrayed the generation-mechanism of GPs, we can model their recombination into luminescent S_1 excitons. Since very few processes are weakly temperature-dependent, we assume that GPs recombine by through-space tunneling and that the distribution of electron–hole distance accounts for the various recombination times. To model this, we assume a distribution of monomolecular recombination rates τ_{GP} and analyze the observed kinetics to recover the probability $P(\tau_{\text{GP}})$ of having a certain lifetime. This can be written as

$$I_{\text{PL}}(t) \propto \sum_{\tau} P(\tau) \frac{e^{-t/\tau}}{\tau} \quad (3)$$

Since $I_{\text{PL}}(t) \propto t^{-1}$, a crude estimate of eq 3 yields a constant value for $P(\tau_{\text{GP}})$. This represents the distribution of lifetimes that are probed over the measurement range (1 ns to 1 ms) and confirms the significant spatial extent of the hole delocalization. A more accurate model, detailed in the Supporting Information, results in the fit shown in Figure 2 and confirms the broad distribution of lifetimes. It is important to note that the slope itself is not a general property of polymers but reflects the energetic landscape probed by GPs in this sample. The fundamental aspect of these observations is that the kinetics are a consequence of the $S_N \rightarrow \text{GP}$ transition, where the S_N has enough excess energy to access many states that would otherwise be separated from S_1 by an energetic barrier.

Having characterized SSA and its byproducts, we now investigate the physical origin of these observations. The high SSA yield is easily explained by looking at quantum-chemical calculations of F8BT, which have shown that the lowest unoccupied molecular orbital (LUMO) is concentrated on the BT unit whereas the highest occupied molecular orbital (HOMO) is delocalized along the backbone of the polymer.²⁹ This is a direct consequence of the D–A nature of this system and results in singlet excitons with a strong charge-transfer character. Consequently, the volume accessible by the hole is significantly larger which, in turn, enhances the likelihood of finding a lower-energy state or other excitations to interact with. The latter results in the high SSA rates observed.⁷

Now that we have explained the role of the D–A nature of the polymer in SSA, we turn to it is consequence on GP formation. We already know that the S_1 -hole is delocalized and

we suspect GP formation to be enhanced with respect to non-D–A polymers because of this. Moreover, S_N states have been calculated to be even more delocalized than their S_1 counterpart in other organic systems.²² This implies that states located further away can be reached. However, this alone can not explain the enhanced GP formation. Extra energy is required to reach all of these supplementary states, and that is precisely why S_N are required. The combination of these two factors, spatial and energetic, implies that the hole can localize much further away from the electron than GPs formed from S_1 . The direct consequence of this is longer-lasting GPs with a larger distribution of lifetimes, such as the ones we are probing in this experiment.

In summary, we have measured room-temperature and 10 K PL of F8BT films as a function of time and fluence, and then successfully modeled our observations. We draw three main conclusions from these results: first, the source of long-lived excitations that repopulate the emissive exciton is SSA, second, these long-lived excitations are electron–hole pairs, and third, they recombine geminately by through-space tunneling resulting in long-lived emission. All of these points are direct consequences of the D–A nature of this polymer and are general considerations that extend well beyond the specific properties of F8BT. This gives us insights into the nature of excitons in other D–A polymers that are now commonly used in photovoltaic applications.

■ EXPERIMENTAL METHODS

The films were spincoated from an *o*-xylene solution onto quartz substrate under N_2 atmosphere in a glovebox. In the time-resolved PL measurements, the sample was measured in a Janus coldfinger cryostat under secondary vacuum (10^{-6} mbar) at RT and 10 K. They were excited by 30 fs pulses at 2.61 eV (TOPAS, light conversion) with a repetition rate of 1 kHz and the collected PL was then measured by a Princeton Instrument ICCD (PI-Max II). In the TA measurements, the samples were excited at 500 Hz by 100 fs pulses at 500 nm, probed at 1 kHz with broadband white-light pulses from a noncollinear parametric amplifier³⁰ and detected with a home-built setup.

■ ASSOCIATED CONTENT

Supporting Information

The full derivation of the model used to fit time-resolved PL data and the fluence-dependent PL intensity are available in a separate document. This material is available free of charge via the Internet at <http://pubs.acs.org/>.

■ AUTHOR INFORMATION

Corresponding Author

*E-mail: sg559@cam.ac.uk.

Notes

The authors declare no competing financial interest.

■ ACKNOWLEDGMENTS

The work was funded by the Natural Sciences and Engineering Research Council of Canada. C.S. also acknowledges funding from the Canada Foundation for Innovation, and the Canada Research Chair in Organic Semiconductor Materials. S.G. acknowledges funding from the Fonds Québécois de Recherche sur la Nature et les Technologies and the UK Engineering and Physical Sciences Research Council. C.S. honours the memory of Paul F. Barbara, who was an important mentor and a friend.

■ REFERENCES

- (1) Chen, H. Y.; Hou, J. H.; Zhang, S. Q.; Liang, Y. Y.; Yang, G. W.; Yang, Y.; Yu, L. P.; Wu, Y.; Li, G. *Nat. Photonics* **2009**, *3*, 649–653.
- (2) Park, S. H.; Roy, A.; Beaupre, S.; Cho, S.; Coates, N.; Moon, J. S.; Moses, D.; Leclerc, M.; Lee, K.; Heeger, A. J. *Nat. Photonics* **2009**, *3*, 297–302.
- (3) Verlaak, S.; Beljonne, D.; Cheyns, D.; Rolin, C.; Linares, M.; Castet, F.; Cornil, J.; Heremans, P. *Adv. Funct. Mater.* **2009**, *19*, 3809–3814.
- (4) Brédas, J.-L.; Norton, J. E.; Cornil, J.; Coropceanu, V. *Molecular Acc. Chem. Res.* **2009**, *42*, 1691–1699.
- (5) Donley, C. L.; Zaumseil, J.; Andreasen, J. W.; Nielsen, M. M.; Sirringhaus, H.; Friend, R. H.; Kim, J.-S. *J. Am. Chem. Soc.* **2005**, *127*, 12890–12899.
- (6) Grey, J. K.; Kim, D. Y.; Donley, C. L.; Miller, W. L.; Kim, J. S.; Silva, C.; Friend, R. H.; Barbara, P. F. *J. Phys. Chem. B* **2006**, *110*, 18898–18903.
- (7) Stevens, M. A.; Silva, C.; Russell, D. M.; Friend, R. H. *Phys. Rev. B* **2001**, *63*, 165213.
- (8) Ai, X.; Beard, M. C.; Knutsen, K. P.; Shaheen, S. E.; Rumbles, G.; Ellingson, R. J. *J. Phys. Chem. B* **2006**, *110*, 25462–25471.
- (9) Paquin, F.; Latini, G.; Sakowicz, M.; Karsenti, P.-L.; Wang, L.; Beljonne, D.; Stingelin, N.; Silva, C. *Phys. Rev. Lett.* **2011**, *106*, 197401.
- (10) Clarke, T. M.; Durrant, J. R. *Chem. Rev.* **2010**, *110*, 6736–6767.
- (11) Cunningham, P. D.; Hayden, L. M. *J. Phys. Chem. C* **2008**, *112*, 7928–7935.
- (12) Piris, J.; Dykstra, T. E.; Bakulin, A. A.; van Loosdrecht, P. H. M.; Knulst, W.; Trinh, M. T.; Schins, J. M.; Siebbeles, L. D. A. *J. Phys. Chem. C* **2009**, *113*, 14500–14506.
- (13) Sheng, C. X.; Tong, M.; Singh, S.; Vardeny, Z. V. *Phys. Rev. B* **2007**, *75*, 085206.
- (14) Silva, C.; Russell, D. M.; Stevens, M. A.; Mackenzie, J. D.; Setayesh, S.; Müllen, K.; Friend, R. H. *Chem. Phys. Lett.* **2000**, *319*, 494–500.
- (15) Köhler, A.; Bässler, H. *Mater. Sci. Eng., R* **2009**, *66*, 71–109.
- (16) Rothe, C.; Hintschich, S. I.; Monkman, A. P. *Phys. Rev. Lett.* **2006**, *96*, 163601.
- (17) Rothe, C.; Monkman, A. P. *Phys. Rev. B* **2003**, *68*, 075208.
- (18) Hertel, D.; Bässler, H.; Guentner, R.; Scherf, U. *J. Chem. Phys.* **2001**, *115*, 10007–10013.
- (19) Hertel, D.; Romanovskii, Y. V.; Schweitzer, B.; Scherf, U.; Bässler, H. *Synth. Met.* **2001**, *116*, 139–143.
- (20) Ohkita, H.; Cook, S.; Ford, T. A.; Greenham, N. C.; Durrant, J. R. *J. Photochem. Photobiol. A* **2006**, *182*, 225–230.
- (21) Ford, T. A.; Ohkita, H.; Cook, S.; Durrant, J. R.; Greenham, N. C. *Chem. Phys. Lett.* **2008**, *454*, 237–241.
- (22) Clark, J.; Nelson, T.; Tretiak, S.; Cirmi, G.; Lanzani, G. *Nat. Phys.* **2012**, *8*, 225–231.
- (23) Gélinas, S.; Pare-Labrosse, O.; Brosseau, C.-N.; Albert-Seifried, S.; McNeill, C. R.; Kirov, K. R.; Howard, I. A.; Leonelli, R.; Friend, R. H.; Silva, C. *J. Phys. Chem. C* **2011**, *115*, 7114–7119.
- (24) Ries, B.; Bässler, H. *J. Mol. Electron.* **1987**, *3*, 15–24.
- (25) Brosseau, C.-N.; Perrin, M.; Silva, C.; Leonelli, R. *Phys. Rev. B* **2010**, *82*, 085305.
- (26) Tachiya, M.; Seki, K. *Appl. Phys. Lett.* **2009**, *94*, 081104.
- (27) King, S. M.; Dai, D.; Rothe, C.; Monkman, A. P. *Phys. Rev. B* **2007**, *76*, 085204.
- (28) Laquai, F.; Im, C.; Kadashchuk, A.; Bässler, H. *Chem. Phys. Lett.* **2003**, *375*, 286–291.
- (29) Kim, J.-S.; Lu, L.; Sreearunothai, P.; Seeley, A.; Yim, K.-H.; Petrozza, A.; Murphy, C. E.; Beljonne, D.; Cornil, J.; Friend, R. H. *J. Am. Chem. Soc.* **2008**, *130*, 13120–13131 PMID: 18767836.
- (30) Cerullo, G.; Silvestri, S. D. Ultrafast optical parametric amplifiers. *Rev. Sci. Instrum.* **2003**, *74*, 1–18.
- (31) We initially attributed this long-lived emission to triplets undergoing TTA in ref 23. However, in light of the experiments and analysis presented in this paper, we now reach the conclusion that they were actually charges.

■ NOTE ADDED AFTER ASAP PUBLICATION

This paper was published on the Web on November 27, 2012. A change has been made to ref 31 and the corrected version was reposted on December 10, 2012.